Exploring climatic and anthropogenic controls on short- versus long-term erosion rates globally

Shiuan-An Chen[1], Katerina Michaelides[1,2,3], David A. Richards[1,2], Michael Bliss Singer[3,4,5]

[1]School of Geographical Sciences, University of Bristol, Bristol, BS8 1SS, UK
[2]Cabot Institute for the Environment, University of Bristol, Bristol, UK
[3]Earth Research Institute, University of California Santa Barbara, Santa Barbara, California 91306, USA
[4]School of Earth and Environmental Sciences, Cardiff University, Cardiff, CF10 3AT, UK
[5]Water Research Institute, Cardiff University, Cardiff, CF10 3AX, UK

Correspondence to: Shiuan-An Chen (b95208027@gmail.com) and Katerina Michaelides (katerina.michaelides@bristol.ac.uk)

Abstract. Erosion is directly tied to landscape evolution through the relationship between sediment flux and vertical lowering of the land surface. Therefore, the analysis of erosion rates across the planet measured over different temporal domains may provide perspectives on the drivers and processes of land surface change over different timescales. Different metrics are commonly used to quantify erosion over timescales of $< 10^1$ y (suspended sediment flux) and 10^3-10^6 y (cosmogenic radionuclides) yet reconciling potentially contrasting rates at these timescales at any location is challenging. Studies over the last several decades into erosion rates and their anthropogenic and climatic controls have yielded valuable insights into geomorphic processes and landforms over time and space, but many are focused at local/regional scales. Gaps remain in understanding large-scale patterns and drivers (climatic, anthropogenic) of erosion across the globe. Here we leverage the expanding availability and coverage of cosmogenic-derived erosion data and historical archives of suspended sediment yield to explore these controls more broadly and place them in the context of classical geomorphic theory. We show that: 1) A relationship, similar to the Langbein-Schumm curve, exists between precipitation and long-term erosion rates, resulting from the balance between rainfall and vegetation cover; 2) There is no systematic relationship between climate indices and short-term erosion rates; 3) Human activities have increased short-term erosion rates, outpacing natural drivers; 4) Across all climatic regions, short-term erosion rates exceed long-term rates, except at locations in mid- and high-latitudes, which inherit the effects of glacial and periglacial processes during ice ages. These results highlight the complex interplay of controlling factors on land surface processes and reinforce the view that timescale of observation reveals different erosion rates and principal controls.

1 Introduction

Sediment yield from drainage basins has been explicitly tied to basin-averaged erosion rate based on an assumed uniform vertical lowering of the land surface in response to sediment export (sediment continuity). Irrespective of the strength of such relationships due to variations and uncertainties in inherent erodibility (e.g., rock strength, etc) and the actual lack of spatial uniformity in basin erosion, drainage basin erosion rates reflect an averaged timescale of landscape evolution in response to

different possible forcing mechanisms. However, the regional controls of climate and anthropogenic activities on erosion over different timescales are not well understood. Despite impressive and increasing collections of long- and short-term erosion rates for drainage basins across the globe, the influences of the prevailing climatic regime and/or anthropogenic activities on basin-averaged erosion rates remains equivocal. Here we leverage existing databases of short-term sediment yield data and long-term cosmogenic radionuclides to explore the relative importance of climate and anthropogenic activities in shaping the landscape around the globe. This analysis has many caveats, since we employ a compilation of previously published datasets, each with its own study objectives, measurement resolutions, potential biases and uncertainties, and regional idiosyncrasies. However, we suggest that a global analysis of existing data, categorised by climatic and anthropogenic masks, may yield new insights into controls on erosion and thus on landscape evolution.

Exploration of the data generated by sediment flux monitoring programmes has revealed insights into the relationships between climatic and anthropogenic drivers and short-term sediment yields. For example, Langbein and Schumm (1958) used a limited dataset of sediment yields to identify a linear relationship between sediment yield and effective mean annual precipitation (MAP) across various biomes in the USA, revealing an erosion peak in the semi-arid rainfall category. They interpreted this result by suggesting that at low MAP, there is also sparse vegetation, so erosion increases commensurately with rainfall via Hortonian overland flow. However, they posit that with sufficient rainfall, vegetation cover also increases, which retards erosion rates because of increased root reinforcement, rainfall interception, higher infiltration, and correspondingly higher evapotranspiration and/or subsurface storm flow (Dunne and Leopold, 1978). Thus, humid regions have lower sediment yields than semi-arid landscapes, despite the higher MAP. Subsequently, Walling and Kleo (1979) extended this analysis to include sediment data from around the globe, censoring the data to basins < 10,000 km^2 to minimise the effects of sediment storage, and including regions with higher MAP than the USA. Their results loosely corroborate the 1958 study, emphasising that sediment yield peaks in dry sub-humid regions, and then apparently peaks again in more humid environments. They suggest that intense precipitation in very humid environments may increase the weathering rate (erodibility) in a manner that exceeds the protection capacity of vegetation cover, leading to a rise of sediment yields. Notably, both papers that analysed short-term sediment yield data put forth reasonable mechanistic arguments, but they are based on either limited data (Langbein and Schumm, 1958) or a 'subjectively fitted curve' through a broad scatter of grouped data (Walling and Kleo, 1979). Given these factors and subsequent debate in the literature (Milliman and Farnsworth, 2013; Walling and Webb, 1996), it seems warranted to revisit the relationship between sediment yields and climate from global data and to extend it to incorporate the increasing database of long-term erosion rates.

In addition to climatic controls, it is well understood that erosion is influenced by anthropogenic activities such as construction, mining, timber harvesting, and conversion of natural vegetation to agriculture (crop and pasture), the latter of which is the most dominant in terms of global land area (Hooke, 2000; Foley et al., 2005). Global analyses of short-term erosion rates from suspended sediment records suggest that agricultural regions have higher erosion rates compared to areas with limited

anthropogenic influences (Dedkov and Mozzherin, 1996; Montgomery, 2007; Wilkinson and Mcelroy, 2007; Kemp et al., 2020). Yet it is unclear how the signal of anthropogenically accelerated erosion is expressed in global sediment records and how it compares with long-term erosion metrics obtained for the same region.

One indication of the relationship between short- and long-term erosion comes from an analysis of co-located erosion rates in the western USA showing that long-term erosion rates are at least an order of magnitude higher than short-term sediment yields (Kirchner et al., 2001). This study argued that episodic large-scale wildfires induce accelerated basin erosion, but they occur on a frequency that is generally not captured by short-term sediment yield records. Large wildfires generally burn the vegetation cover, deposit unconsolidated material on hillslopes, destroy plant roots, decrease infiltration rates, and therefore create a more erodible landscape susceptible to debris flows and landslides, which may increase the erosion rate of drainage basins over longer timescales (Cannon et al., 1998; Meyer et al., 2001; Pierce et al., 2004). However, despite the prevalence of extensive glaciation in the montane western USA, the Kirchner et al. (2001) study did not address the role of past glacial and periglacial erosion on their measured long-term erosion rates. Glaciers erode bedrock via quarrying and abrasion wherever subglacial conditions allow basal sliding, and through freeze–thaw and weathering processes on the margins of ice (Ganti et al., 2016; Harel et al., 2016; Cook et al., 2020; Delunel et al., 2020). Glacial and periglacial erosion has been shown to increase long-term erosion rates in temperate and cold regions, especially within mid- and high-latitudes (Portenga and Bierman, 2011; Harel et al., 2016). It is possible that erosion due to glaciers over large areas may have been a major contributor to the higher long-term erosion rates measured for the Idaho sites in Kirchner et al. (2001). What is clear is that both glaciers and episodic wildfires have the potential to increase long-term erosion rates relative to short-term sediment yields under natural conditions (i.e., in the absence of significant anthropogenic activities), yet the relationship between erosion and climate on longer timescales is unclear.

A previous study investigated global patterns of long-term erosion rates based on a compilation of ^{10}Be measurements (n = 1,790) showed a non-linear relationship (3rd order polynomial) between MAP and erosion rate, which is characterised by an increase in erosion rate to a local maximum MAP at ~ 1,000 mm, followed by a slight reduction up to MAP of ~ 2,200 mm, and subsequently a return to increasing values for higher MAP (Mishra et al., 2019). Despite significant scatter in the data and a questionable fit of the polynomial peaks to the data (e.g. Fig. 4 in Mishra et al., 2019 seems to show a peak in the erosion data for semi-arid rainfall but their fitted polynomial curve places the peak at 1000 mm), the authors explain the relationship by similar mechanisms presented by the previous short-term studies s (e.g. Langbein and Schumm, 1958), despite notable differences in their relative patterns of erosion rate with MAP. Clearly, there are remaining uncertainties about the role of precipitation regimes in controlling long-term erosion rates, especially given potential mismatches between the timescales of MAP and erosion measurement, as well as the proliferation of cosmogenic data across the globe.

Finally, we would be remiss to ignore the role of tectonics and lithology in affecting both topography and erosion rates, since numerous studies have shown erosion rates are positively correlated to total basin relief and slope gradient, tectonic uplift rates, and the erodibility of lithology, for both short-term (Milliman and Meade, 1983; Milliman and Syvitski, 1992; Summerfield and Hulton, 1994; Aalto et al., 2006; Syvitski and Milliman, 2007; Milliman and Farnsworth, 2011; Yizhou et al., 2014) and long-term erosion rates (Granger et al., 1996; Bierman and Caffee, 2001; Schaller et al., 2001; von Blanckenburg, 2006; Binnie et al., 2007; Dibiase et al., 2010; Portenga and Bierman, 2011; Wittmann et al., 2011; Covault et al., 2013; Codilean et al., 2014; Harel et al., 2016; Schmidt et al., 2016; Grin et al., 2018; Struck et al., 2018; Tofelde et al., 2018; Hilley et al., 2019). Therefore, we investigate correlations between erosion rates and key topographic indicators of tectonics and lithology to reveal the broad associated patterns across the globe, but we focus most of our work on the influence of climate (including climate classifications, MAP, glaciers) and anthropogenic activities (agricultural land use categories).

This study aims to understand the geographic expression of long- and short-term erosion rates around the globe and explore climatic and anthropogenic controls on erosion rates. We specifically address the following key questions: 1) What is the overall pattern of long- and short-term erosion rates categorised by climate regimes? 2) To what extent do long-term erosion rates reflect glacial (and periglacial) processes in mid- and high-latitude regions? 3) Are previously theorised relationships between precipitation and erosion rate applicable to both short and long timescales? 4) How do anthropogenic activities affect short-term erosion rates?

2 Erosion proxies

To explore spatial and temporal patterns in erosion rates, we need proxies for erosion rates that capture processes at different timescales and sufficient data from global geographic and climatic regions. Two key proxies used to represent erosion in geomorphology are: suspended sediment yields for short-term rates (10^0-10^1 yr), and in-situ cosmogenic radionuclides for long-term basin-averaged erosion rates (10^3-10^6 yr). While each of these proxies is associated with different assumptions and different inherent uncertainties, they are commonly used in geomorphology to investigate spatial and temporal changes in erosion in response to climatic and tectonic forcing (Clapp et al., 2001; Pan et al., 2010; Wittmann et al., 2011; Yizhou et al., 2014), to compare erosions rates between basins (Milliman and Meade, 1983; Milliman and Syvitski, 1992; Summerfield and Hulton, 1994; Dedkov and Mozzherin, 1996; Portenga and Bierman, 2011; Harel et al., 2016), and to investigate potential drivers of erosion at different time scales (Kirchner et al., 2001; Schaller et al., 2001; Covault et al., 2013; Ganti et al., 2016; Delunel et al., 2020).

Erosion rates calculated from suspended sediment yield are calculated by measuring the sediment concentration and discharge at a gauging station over years to decades, and then converting their product into mean annual sediment flux, then to sediment yield (t ha^{-1} yr^{-1}) normalised by upstream drainage area, and subsequently to erosion rate (mm yr^{-1}), assuming a basin-averaged

soil bulk density. This method provides an averaged value of erosion rate for the upstream area that neglects the storage of sediment during transportation and only accounts for sediment transported as suspended load, which makes up the majority of sediment export from basins around the world (Leopold et al., 1964). The method neglects any sediment transported as bedload or dissolved load. The omission of bedload and dissolved load data may underestimate basin-averaged erosion rates slightly, but these data are too scarce, and too uneven to meta-analyse between climate zones at the global scale. A meaningful, systematic correction of short-term erosion rates is not possible due to variations in the controls on the type of sediment load between basins. For example, the percentage of bedload to the total load tends to be higher in mountain regions and drylands (Dedkov and Mozzherin, 1996; Singer and Dunne, 2004), but the percentage of dissolved load seems to be higher in tropical regions and lower in drylands (Milliman and Farnsworth, 2011). Previous studies estimated that the bedload typically accounts for < 10% of the total load (Milliman and Meade, 1983), and the average dissolved load is even less but with significant variation (Milliman and Farnsworth, 2011). For example, in some dryland basins, dissolved load is as low as ~ 0.2% (Alexandrov et al., 2009). Despite this limitation, suspended sediment yield provides a record of recent responses within landscapes to climatic and/or anthropogenic forcing (Walling and Webb, 1996; Walling and Fang, 2003) and is used widely as a reliable erosion proxy.

In-situ cosmogenic radionuclides such as Beryllium-10 (^{10}Be) and Aluminium-26 (^{26}Al), are produced by the interaction of secondary cosmic rays with minerals in rocks and soils in the uppermost few metres of the Earth's surface. The concentration of cosmogenic radionuclides near the surface is principally a function of the production rate, radioactive decay rate and erosion rate (or rate of surface stripping). Therefore, the concentration of cosmogenic radionuclides in river sediments can be used for estimating basin-averaged erosion rates, and the timescale of the estimation depends on the erosion rate itself (i.e. the time taken to lower the land surface) (Brown et al., 1995; Granger et al., 1996; Granger et al., 2013; Granger and Schaller, 2014; von Blanckenburg and Willenbring, 2014). This method, when applied to riverine sediments, also provides an averaged erosion rate that is insensitive to short-term sediment storage within the upstream basin. Furthermore, this method is more practicable in basins where the land surface has been subject to continuous exposure to cosmic rays and long-term steady erosion (i.e. where abrupt and deep erosion, and long-term burial followed by erosion are minimum) (Brown et al., 1995; Granger et al., 2013; Dosseto and Schaller, 2016; Struck et al., 2018). Erosion rates estimated using cosmogenic nuclides represent longer timescales than suspended sediment records (10^3–10^6 yr versus 10^0–10^1 yr), and are therefore suitable for analysing the influences of climate and tectonics, while being insensitive to the influences of anthropogenic activities or recent episodic erosion events with shallow erosional depth (Brown et al., 1995; von Blanckenburg, 2006; Granger et al., 2013; Granger and Schaller, 2014; Dosseto and Schaller, 2016).

We note several uncertainties and assumptions inherent in the use of ^{10}Be-derived erosion rates. The main assumptions are that: 1) catchments have been receiving cosmic rays throughout the time they have been eroding the layer that has moved through the basin to the channel; 2) eroded sediment is coming from the near surface (i.e. minimal contribution of shielded

sediments from deep-seated landslides); and 3) erosional processes are steady and uniform in the upstream basin. These assumptions may not hold if a catchment has been glaciated (or if only part of it has been glaciated). Despite these limitations and with these caveats in mind, in this study we deem any ^{10}Be-derived erosion data obtained from published data sources to be suitable for assessing broad differences in erosion rates across landscapes between climate zones given that the original measurements were obtained to estimate erosion rates in these glaciated basins. Finally, the timescale of ^{10}Be-derived erosion rate depends on the erosion rate itself and it may be averaged over glacial and/or non-glacial periods, so formerly glaciated regions may not have experienced the last Ice Age directly. However, former glaciation generally enhances sediment production leading to higher transport rates by subsequent fluvial processes during warmer periods (Ganti et al., 2016).

3 Methods

Our analysis is based on a compilation of long- and short-term drainage basin erosion rates across the globe from existing databases and published literature (see Data availability). Data were stratified by the Köppen–Geiger (K–G) climate classification and the Aridity Index (AI) classification to explore potential climatic controls. We also explore the influence of glacial and periglacial regions at the last glacial maximum (LGM; Ray and Adams, 2001), mean slope gradient and total relief of river channels (extracted and calculated from Global Longitudinal Profiles database, GLoPro; Chen et al., 2019), and the spatial pattern of agricultural regions as a proxy for anthropogenic activity (Foley et al., 2005). Additionally, for comparison with earlier studies, we explore variation in erosion rates against MAP across the continental USA obtained from gauge data (calculated from CPC US Unified Precipitation data, https://psl.noaa.gov/data/gridded/data.unified.daily.conus.html).

Long-term erosion rates were obtained from the Open Cosmogenic Isotope and Luminescence Database (OCTOPUS, https://earth.uow.edu.au/), which reports basin-averaged erosion rates derived from cosmogenic nuclides (^{10}Be and ^{26}Al) and luminescence measurements in fluvial sediments (Codilean et al., 2018). This database classifies data based on the methods, regions, and degree of completeness. To gain the highest reliability and consistency, we only included ^{10}Be-derived erosion rates of CRN (cosmogenic radionuclide) International and CRN Australia categories from the database, resulting in a total of 3,074 data points (Fig. 1). For each data point, we extracted the erosion rate, coordinates, and drainage basin area.

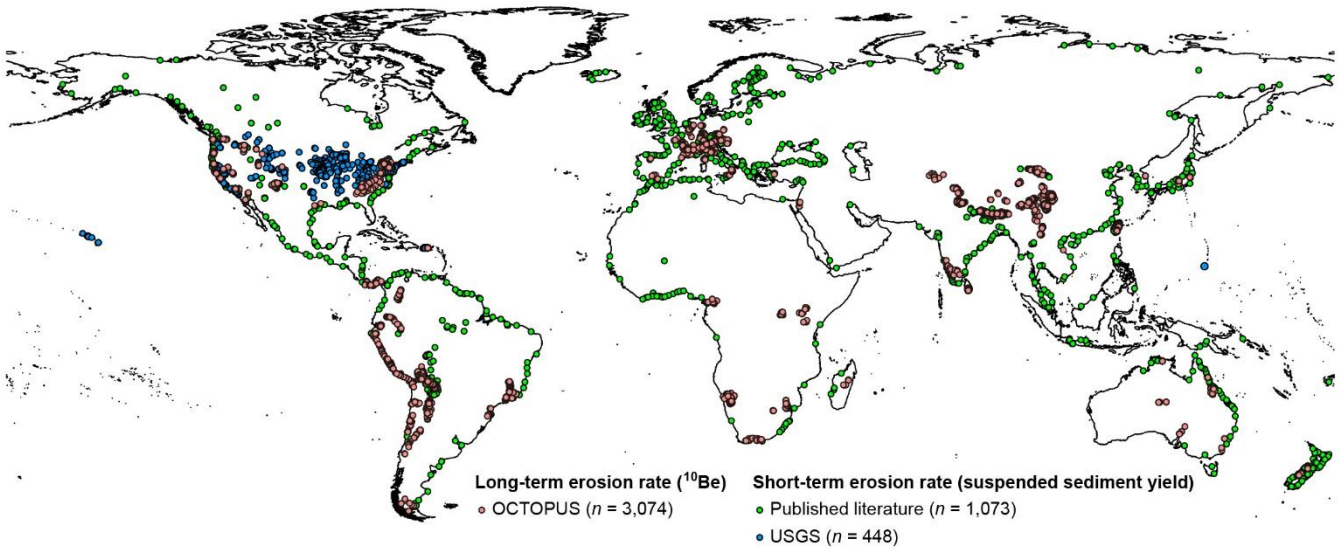

Figure 1: Global map of drainage basin erosion rate locations. Long-term erosion rates were obtained from OCTOPUS (Open Cosmogenic Isotope and Luminescence Database, red), estimated by ^{10}Be in the fluvial sediments. Short-term erosion rates were compiled from published literature (green) and USGS (blue), determined by suspended sediment yield of gauging stations. Coastline is from Nature Earth (https://www.naturalearthdata.com) in the Pseudo Plate Carree map projection.

Short-term erosion rates were compiled from published studies and the USGS (National Water Information System, https://waterdata.usgs.gov/nwis), based on estimations from suspended sediment yields at gauging stations (see Data availability). From these published studies, we compiled sediment yields (t ha^{-1} y^{-1}) or erosion rates (mm ky^{-1}) at each data point. To convert erosion rates from sediment yields, we assumed sediment density to be 1.6 g cm^{-3} (= 1.6 t m^{-3}). Using this density, sediments with a depth of 0.1 mm across an area of 1 ha, have a mass of 1.6 t. A sediment yield of 1 t ha^{-1} y^{-1}, for example, is equivalent to an erosion rate of 0.0625 mm y^{-1} (or 62.5 mm ky^{-1}). If the coordinates of the gauging stations were not provided, we acquired the point coordinates from Google Maps. If data from the same gauging station were reported in multiple literature sources, we only included the erosion rate with the most recent data record. For the USGS data, two criteria were set for choosing gauging station data: 1) monitoring time period > 5 years, and 2) basin area < 2,500 km^2. The reason for the area threshold in the USGS data is to compensate for the generally larger basin sizes in the non-USGS datasets and to enable comparison to the long-term erosion rates (i.e. from the OCTOPUS database), which were typically obtained from smaller drainage basins. Note that some of the gauging stations meeting these criteria may be on the same river. We extracted the daily sediment discharge (t d^{-1}), converted this into sediment yield (t ha^{-1} y^{-1}) by summing the daily data and dividing by the number of years and basin area. The sediment yield was then converted into an erosion rate.

The USGS data are quality checked before being released by the organisation, but suspended sediment yield data compiled from peer-reviewed literature cannot be quality controlled for consistency. Therefore, uncertainty ranges will be highly

variable for several reasons (Milliman and Farnsworth, 2011): the variety of measuring techniques over different periods of time; inadequate monitoring period (i.e. several rivers with historic records < 5 years); watershed modification (e.g. resulting from dam construction or climate change); variable sediment densities across basins; and potentially erroneous transcription of the data. We have tried to reduce data uncertainties as far as possible by focusing on published sediment flux values from highly cited and well-regarded studies, which contain descriptions of data quality control. In total, we obtained 1,521 short-term erosion rates; 1,073 from published studies and 448 from USGS (Fig. 1), with corresponding station coordinates and drainage basin areas (see Data availability).

We use two climate classifications in our analysis of the global short- and long-term erosion data: 1) The K–G climate classification, which is based on biome types defined by temperature and precipitation thresholds. Here we adopt the most updated version of K–G (Peel et al., 2007), which includes five main zones (Tropical, Arid, Temperate, Cold, and Polar) and 29 sub-zones. We classified erosion rates into the main K–G zones to provide sufficient data points in each category, but we excluded the Polar zone because there are too few data. 2) The AI is a quantitative metric for characterising the average water balance, calculated by dividing MAP by mean annual potential evapotranspiration (PET) from the Global Aridity and PET Database (Trabucco and Zomer, 2009). For ease of statistical comparison, we adopted a categorical approach and used the following thresholds for the AI: Hyper-arid (< 0.03), Arid (0.03–0.2), Semi-arid (0.2–0.5), Dry sub-humid (0.5–0.65), and Humid (> 0.65).

The extent of glacial and periglacial processes for the primary Ice Ages was determined from Ray and Adams (2001), which provides the global vegetation map at the LGM (25,000–15,000 BP) based on fossil and sedimentary information, and expert consultation. The glacial and periglacial regions at the LGM were defined as the following five categories in Ray and Adams (2001): Tundra, Steppe-tundra, Polar and alpine desert, Alpine tundra, and Ice sheet and other permanent ice. Since the timescale of ^{10}Be-derived erosion rates is in the range of 10^3–10^6 years, the data cover several glacial–interglacial cycles. Nevertheless, we used glacial coverage at the LGM as the most reliable estimate of glacial influences erosion across our study regions.

Anthropogenically impacted regions were determined from Foley et al. (2005), which provides global maps of croplands, and pastures and rangelands classified by the relative percentages of areas within these land uses. These maps were modified from previous studies (Ramankutty and Foley, 1999; Asner et al., 2004), in which they classified land use types from satellite images using GIS analysis. We conservatively defined anthropogenic regions with > 50% area of croplands or pastures and rangelands.

MAP data for the continental USA from CPC US Unified Precipitation data are in raster format with 0.25-degree resolution (~28 km at the equator), including daily precipitation rates from 1948 to 2006 (59 years). We summed the daily data of each grid cell in each year to convert daily data into yearly data and calculated the precipitation rates for all locations where we

have erosion rates. We constrained our analysis of MAP to the USA because of the quality and consistency of the gauge data which are lacking at the global scale. For the global scale analysis, we use K–G and AI climate classifications as proxies for rainfall regimes.

The topographic parameters used here include the mean slope gradient and total relief of entire river longitudinal profiles extracted from the GLoPro database (Chen et al., 2019). GLoPro includes river longitudinal profiles around the globe which were extracted from NASA's 30 m Shuttle Radar Topography Mission Digital Elevation Model (SRTM–DEM). The rivers in the database are the mainstem rivers (the longest rivers) of basins or sub-basins that do not cross K–G climate sub-zones. The database contains topographic data include the concavity, elevation, flow distance, and drainage area of each river profile. To extract river profiles from the database for comparing topographic parameters with erosion rates, we chose a subjective distance threshold of 150 m between river profiles and erosion rate sampling points (i.e. selecting river profiles which are within 150 m to the closest erosion rate point). We then calculated the mean channel gradient and total channel relief of each river longitudinal profile for our erosion points, which is broadly representative of the topographic influences on erosion rate inherited from tectonics and lithology.

To analyse the statistical difference in erosion rates between climate zones, timescales, and environmental controls, we used the Kruskal–Wallis hypothesis test. The Kruskal–Wallis is a nonparametric hypothesis test that compares the values of multiple samples to determine whether they are from the same distribution, which is useful for cases where the data may not be normally distributed. The purpose here is to identify differences between categories of data rather than not to investigate complex relationships between environmental controls. The test was conducted by the built-in function, kruskalwallis, in MATLAB R2018a.

4 Results

4.1 Climate influence on long- and short-term erosion rates

Short-term erosion rates are significantly higher ($P < 0.05$) than long-term rates in all climate zones, except for the Cold K–G zone (Fig. 2, Table 1a). Within the AI categories, there is a general pattern of an increasing difference between long- and short-term erosion rates with higher aridity. However, these differences are only significant for the Arid and Semi-arid categories ($P < 0.05$, Fig. 2b, Table 1b).

For the long-term erosion rates, Tropical and Arid K–G zones have significantly ($P < 0.01$) lower erosion rates (medians = 29.7 and 32.2 mm kyr^{-1}, respectively) than Temperate and Cold zones (medians = 92.9 and 92.5 mm kyr^{-1}, respectively, Fig. 2a, Table 1a). Within the AI categories, long-term erosion rates are significantly lower in drier regions (i.e. Hyper-arid, Arid, and Semi-arid group of categories) compared to more humid regions (i.e. Dry sub-humid and Humid group of categories, $P <$

0.01) (Fig. 2b), and there are no differences within them ($P > 0.05$, Table 1b). The maximum long-term erosion rates occur in the Temperate and Cold K–G categories and in the Dry sub-humid AI category.

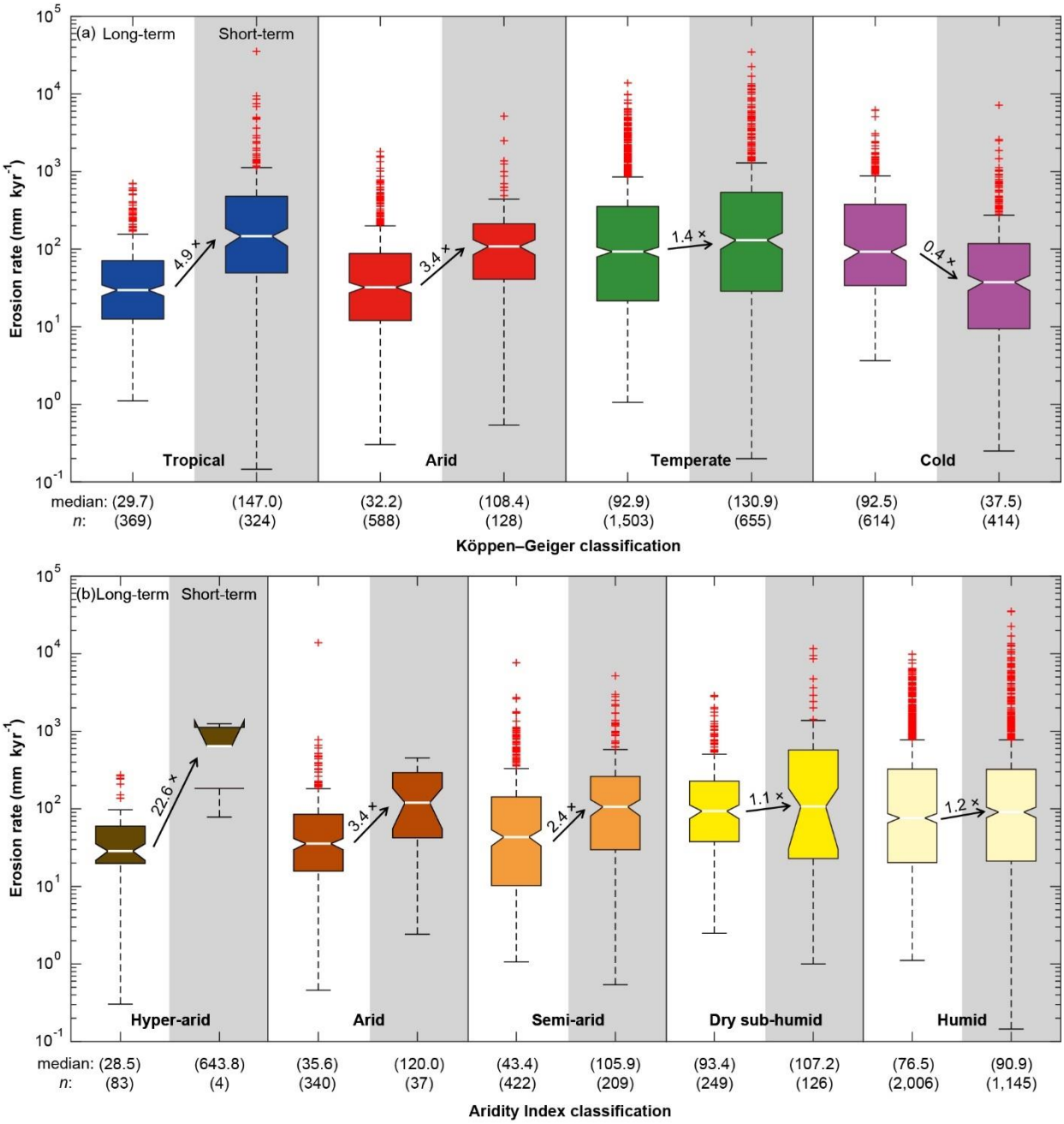

Figure 2: Long- and short-term erosion rates for climate zones of Köppen–Geiger climate classification (a) and Aridity Index classification (b). Boxplots with white backgrounds contain the long-term rates, whilst those with the grey backgrounds contain short-term rates. For each box, the central line indicates the median value, and the bottom and top edges indicate the 25th and 75th percentiles, respectively. The notch represents the range of the median at the 95% significant level (note that the lower notch of short-term erosion rates of Hyper-arid category extends beyond the range of y-axis due to the limited number of samples in this category). Red crosses represent outliers. The arrows and numbers between boxplots in each climate zone indicate the trends and ratios of median values for short- to long-term rates ($R_{S/L}$). Median values and the number of data points for each distribution are listed below the x-axis.

Table 1: *P*-values of Kruskal–Wallis tests comparing long-term (n = 3,074) and short-term (n = 1,521) erosion rates between climate zones of Köppen–Geiger climate classification (a) and Aridity Index classification (b), and between long- and short-term erosion rates of each climate zone. Bold numbers indicate significant *P*-values (< 0.05). The number of data points for each climate zone is listed in Fig. 2.

(a)

Long-term rates comparison			
	Arid	Temperate	Cold
Tropical	0.88	**<0.001**	**<0.001**
Arid		**<0.001**	**<0.001**
Temperate			0.54

Short-term rates comparison			
	Arid	Temperate	Cold
Tropical	0.42	0.95	**<0.001**
Arid		0.82	**<0.001**
Temperate			**<0.001**

Long- and short-term rates comparison	
Tropical	**<0.001**
Arid	**<0.001**
Temperate	**0.02**
Cold	**<0.001**

(b)

Long-term rates comparison				
	Arid	Semi-arid	Dry sub-humid	Humid
Hyper-arid	0.97	0.40	**<0.001**	**<0.001**
Arid		0.75	**<0.001**	**<0.001**
Semi-arid			**<0.001**	**<0.001**
Dry sub-humid				0.53

Short-term rates comparison				
	Arid	Semi-arid	Dry sub-humid	Humid
Hyper-arid	0.88	0.79	0.88	0.73
Arid		1	1	1
Semi-arid			1	1
Dry sub-humid				0.95

Long- and short-term rates comparison	
Hyper-arid	0.07
Arid	**0.02**
Semi-arid	**<0.001**
Dry sub-humid	1
Humid	1

For comparability to other studies, we also plotted long-term erosion rates against MAP for all data points within the continental USA. A trend through the data was fitted by the LOWESS smoothing method, which uses locally weighted linear polynomial regression by neighbouring data points to smooth data (Cleveland, 1979). We fitted the regression using the built-

in function, smooth, in Matlab, to highlight the pattern of erosion rates. We set the LOWESS polynomial as "linear", the span as "30% of data points", and the robust option as "off". We also provide the uncertainty range based on the mean error of long-term erosion rates reported in the OCTOPUS database. The resulting curve shows a pattern of erosion rates with MAP similar to that shown for AI (Fig. 2b), with the highest erosion rates exhibited in the Dry sub-humid category (MAP ~ 600 mm, Fig. 3a), followed by a dip around 1,250 mm and a subsequent increase again in erosion rates in more humid regions (MAP > 1,300 mm).

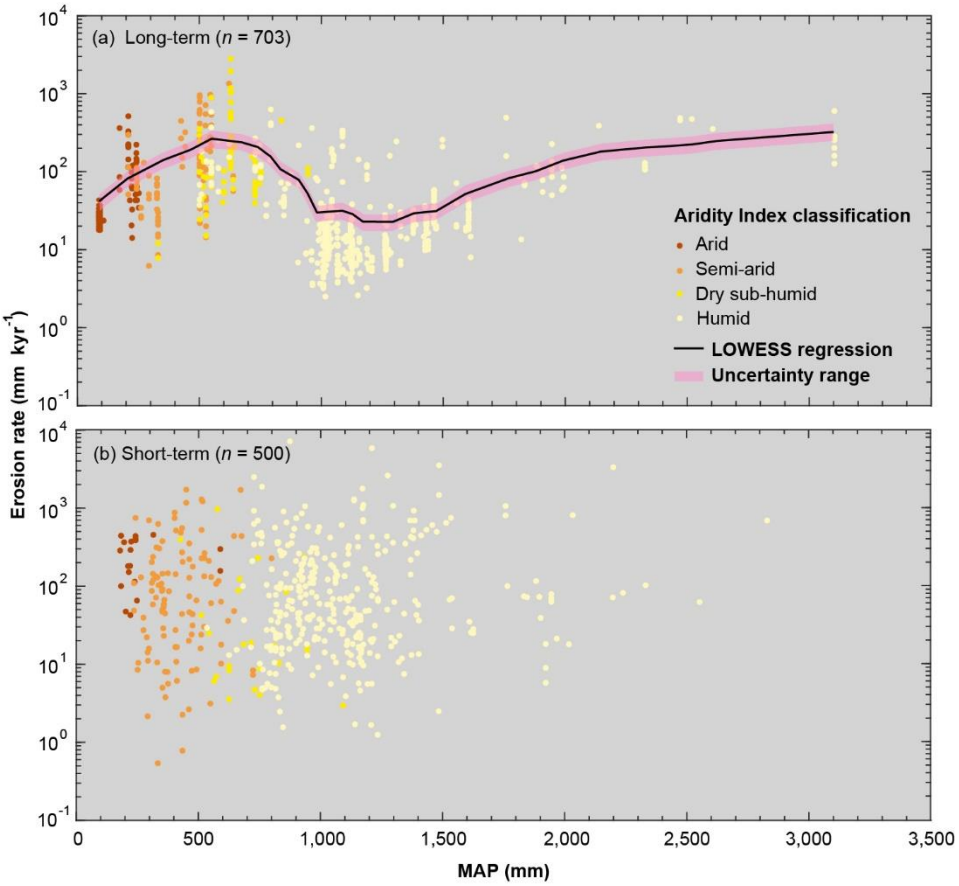

Figure 3: Relationships between mean annual precipitation (MAP) and long- (a) and short-term (b) erosion rates in the USA. Points are colour coded by Aridity Index categories. Black curve in panel a is LOWESS regression, and the pink shading represents the approximate average uncertainty in the long-term erosion rates.

Within the short-term erosion rates, there is no apparent dependency on climate according to either climate classifications ($P > 0.05$), except in the Cold zone of K–G classification, where there were significantly lower erosion rates compared to other climate zones ($P < 0.01$, Fig. 2a, b, Table 1). The medians of short-term erosion rates in all climates are generally between 90 and 150 mm kyr^{-1}, whereas the Cold K–G zone is only 37.5 mm kyr^{-1}, and the Hyper-arid AI category is as high as 643.8 mm

kyr^{-1} (note that the result of Hyper-arid category may not be robust because of limited available data). Similarly, there is no apparent relationship between short-term erosion rates and MAP for the continental USA (Fig. 3b).

4.2 Influence of glaciation on long-term erosion rates

To explore the influence of past glaciations on long-term erosion rates, we compared data for those locations that are currently in the Temperate K–G zone and were previously in glacial and periglacial zones during the Pleistocene (e.g. north-western Europe, part of the Andes, the Himalayas, and New Zealand) against the Temperate sites that were not glaciated (Fig. 4), based on the work of Ray and Adams (2001). We find that the median long-term erosion rate for formerly glaciated regions of the Temperature zone is approximately 5 times higher than in non-glaciated regions (medians = 202.3 and 41.4 mm kyr^{-1}, respectively, $P < 0.01$). This result confirms the role of glacial and periglacial influences, such as glacier, freeze–thaw, and weathering processes, in shaping surface across the landscape resulting in higher long-term erosion rates.

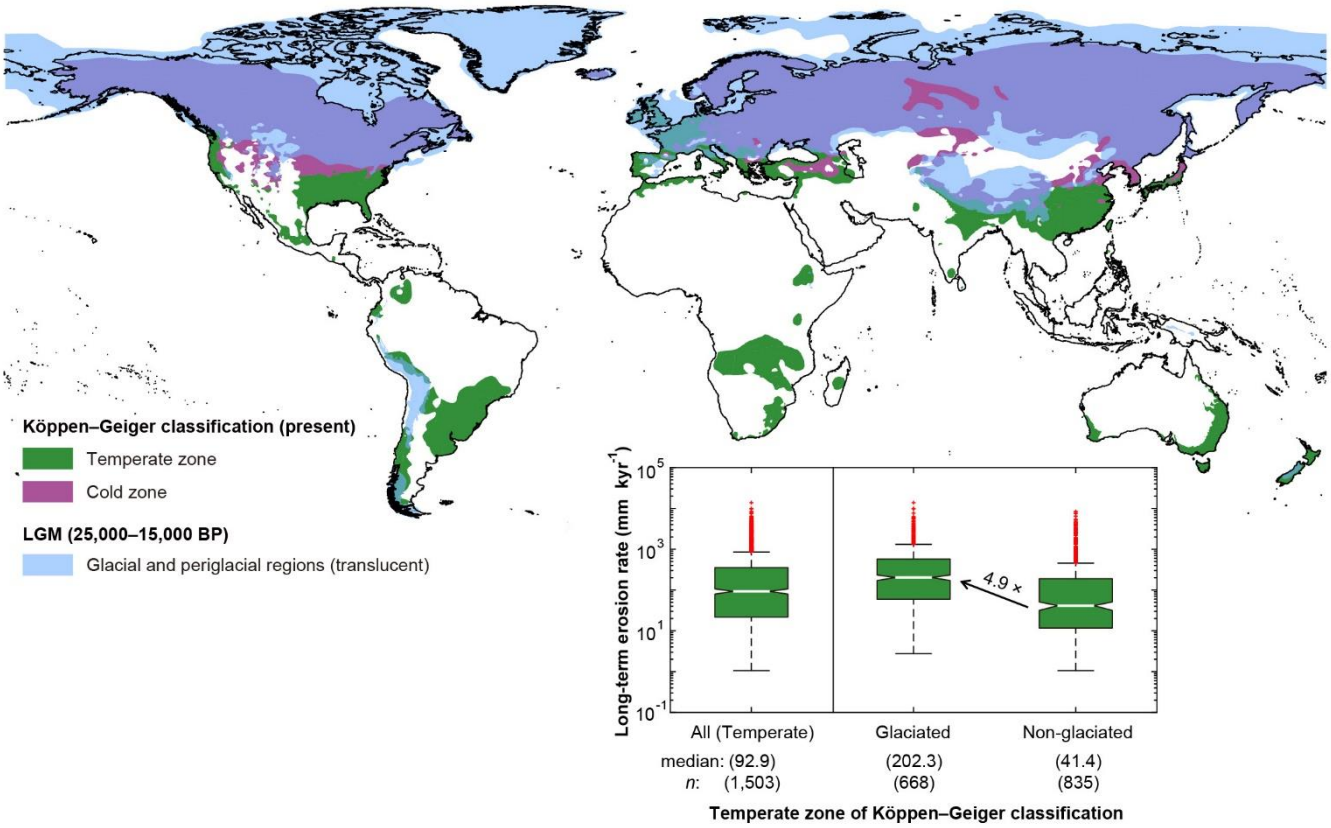

Figure 4: The extent of glacial and periglacial regions at the last glacial maximum (LGM) and the area of Temperate and Cold zones of Köppen–Geiger climate classification in the present. The glacial and periglacial regions were drawn from Ray and Adams (2001), according to the description in Methods. The inset panel compares long-term erosion rates in the Temperate K–G zone with and without glacial influences at the LGM, indicating 4.9 times higher median erosion rates in formerly glaciated regions compared to non-glaciated regions.

4.3 Anthropogenic influences on short-term erosion rates

Anthropogenic influences on short-term erosion rates were examined using land use as a proxy. We compared the erosion rates in classified 'croplands', and 'pastures and rangelands' (from Foley et al., 2005), against erosion rates in regions with no evidence of anthropogenic disturbance in land use. The median short-term erosion rate for these agriculturally influenced areas is 1.4 times higher than in regions without these anthropogenic influences (78.3 mm kyr^{-1}, $P < 0.05$, Fig. 5). However, there was no significant difference in erosion rates between these two types of anthropogenically impacted land uses (104.2 and 114.0 mm kyr^{-1}, respectively, $P > 0.05$).

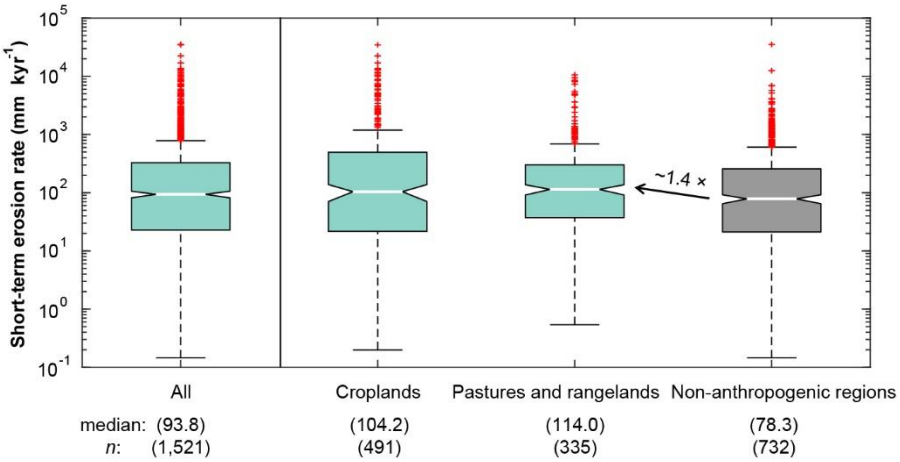

Figure 5: The comparison of global short-term erosion rates with and without anthropogenic influences. The extent of croplands and pastures and rangelands were digitised from Foley et al. (2005), and the figure shows that short-term erosion rates with anthropogenic influences are ~1.4 times higher than in non-anthropogenically impacted regions.

4.4 Influence of basin topography

Finally, we explored the influences of basin area and topography on erosion rates. Across the whole dataset, for both long- and short-term erosion rates, there is no clear relationship with basin area (Fig. 6). To investigate this further, we grouped the erosion rates in three bins of basin area, < 500 km^2, 500–2,500 km^2, and ≥ 2,500 km^2. The area thresholds were chosen to achieve a similar number of observations within each bin and climate category. We then calculated the ratio of short- to long-term median erosion rates ($R_{S/L}$). We found a negative relationship between $R_{S/L}$ and basin area for each K–G climate zone, except the Cold zone (Fig. 7). Generally, short-term erosion rates are several times higher than long-term rates in small basins, whilst in large basins, long-term rates tend to be more similar or even higher than short-term rates. In addition, long-term erosion rates are positively related to channel gradient and channel relief (R^2 = 0.29 and 0.24, respectively; P < 0.01), whilst for short-term erosion rates, the influences of these topographic parameters are unclear (Fig. 8).

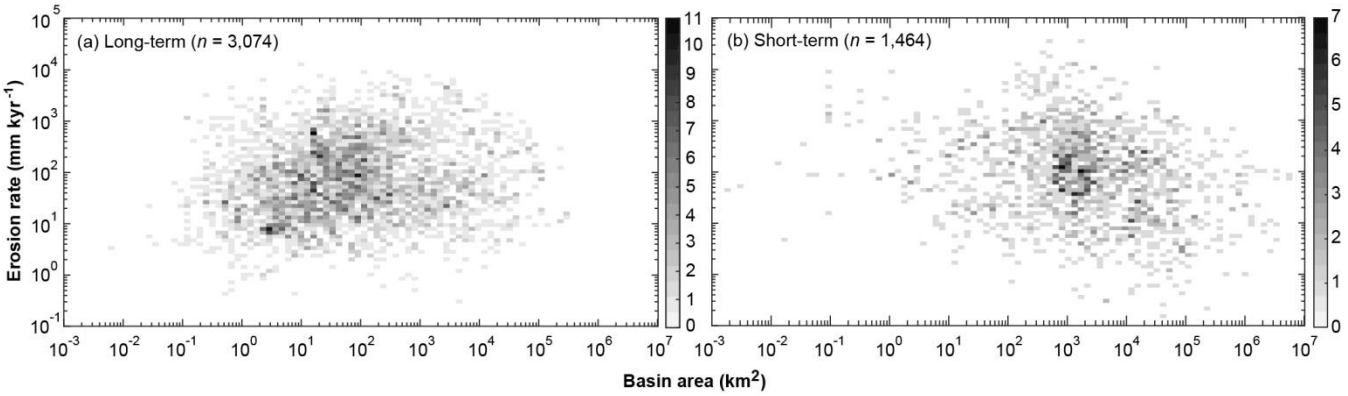

Figure 6: Density scatter plots of the drainage basin area v. long- (a) and short-term (b) erosion rates. The colour ramp indicates the number of data points in each pixel.

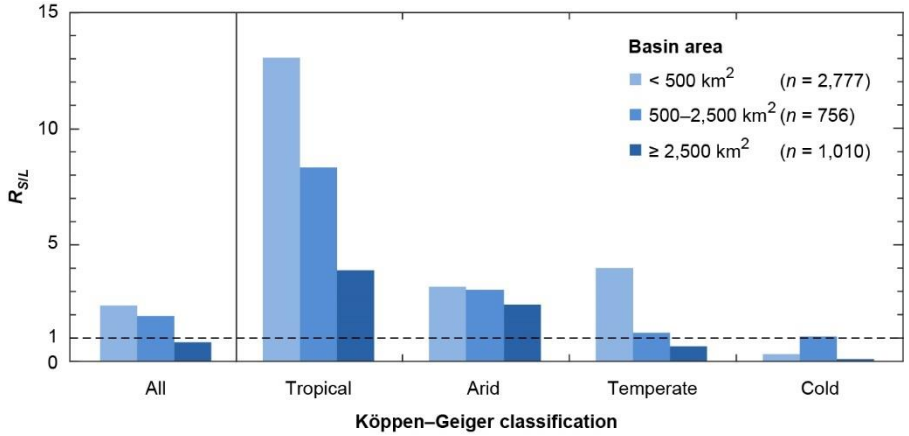

Figure 7: The ratio of short- to long-term erosion rates ($R_{S/L}$) of each basin area bin between climate zones for the Köppen–Geiger climate classification. Each ratio was calculated from the medians of short- to long-term erosion rates of each area bin in each climate zone. The numbers of data points in each basin area bin (short-term plus long-term erosion rates) are listed in the legend. The dotted line indicates equality of short- and long-term rates. Generally, in smaller basins, short-term erosion rates tend to be higher than long-term rates compared to larger basins.

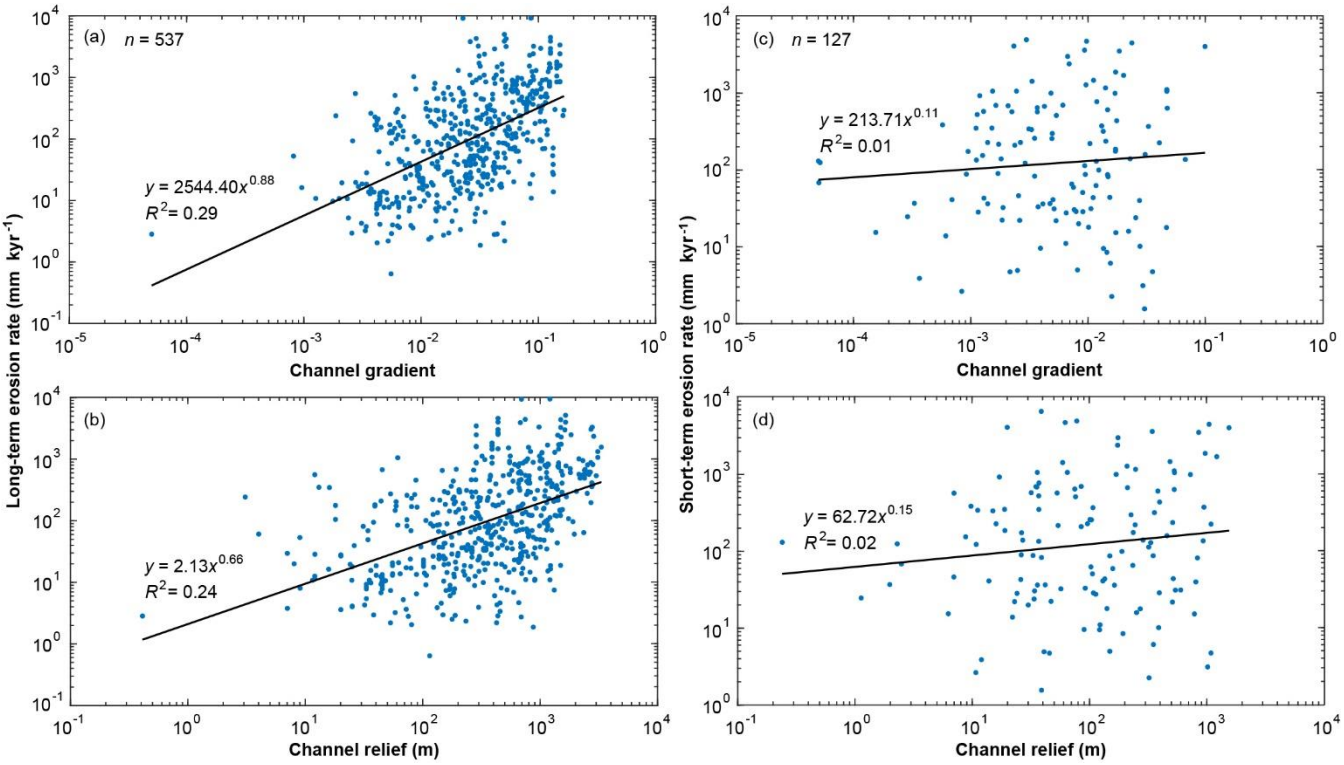

Figure 8: Relationships between topographic parameters of river longitudinal profiles and long- (a, b) and short-term (c, d) erosion rates.

5 Discussion

We set out to investigate the key potential drivers of erosion and their influence on erosion rates over short ($<10^1$ y) and long (10^3 – 10^6 y) timescales, and we compared rates between these timescales for each climate classification. We specifically investigated erosion rate variations through the lenses of climate (classifying by Köppen-Geiger and Aridity Index classifications, mean annual precipitation, and historical maps of glaciated v. non-glaciated regions), anthropogenic activities (classified agricultural regions), and basin topography (channel gradient and channel relief). We fully acknowledge that drainage basin erosion rates are controlled by various (sometimes interrelated) factors, some of which may compound erosion at a particular site (e.g. high rainfall regime with intensive land use), and some of which may offset each other (e.g. agricultural activities may accelerate erosion in lowland areas where erosion rates would be expected to be low under undisturbed conditions). We also recognise the inherent uncertainties and biases in the underlying data used in our analyses, since we relied on public databases. Nevertheless, our analysis reveals important differences in short- versus long-term erosion rates after stratification by various climatic indices and human impacts on the landscape. This comparison of erosion rates for distinct timescales has been addressed at particular locations (Clapp et al., 2000; Kirchner et al., 2001; Gellis et al., 2004; von Blanckenburg, 2006; Kemp et al., 2020), but has not been carried out on a global basis, at which stratification by climate and

anthropogenic drivers is possible. Some of our research results corroborate prior studies, but there are several novel results that have emerged from the analysis. We highlight both below with emphasis on the new findings.

A key finding from this meta-analysis of global data is that there is a relationship between long-term erosion rates and climate (Figs. 2b, 3a), which broadly corroborates early theoretical work on short-term erosion rates from sediment yields (Fig. 9; Langbein and Schumm, 1958; Walling and Kleo, 1979) and modelling investigation (Collins and Bras, 2008; Istanbulluoglu and Bras, 2006). Based on a small number of grouped data points from the USA, Langbein and Schumm (1958) proposed that sediment yields peak in semi-arid regions due to the combination of rainfall (high enough) and vegetation cover (low enough) that results in optimum conditions for erosion (Fig. 9). Note that for direct comparison with other data, we have replotted the original Langbein-Schumm curve adjusting their effective precipitation (determined based on runoff) to MAP by assuming 50% losses (0.5 runoff coefficient) of incoming precipitation, which shifts their erosion peak to the dry sub-humid precipitation regime (MAP: 500 – 800 mm/y). Following Langbein-Schumm, Walling and Kleo (1979) found a similar erosion peak in Dry sub-humid regions (MAP ≈ 600), they also identified two further peaks in sediment yield in humid regions, where precipitation may be particularly intense and weathering (erodibility) may be high (Fig. 9), although the authors acknowledged that their fit to data points was subjective.

Remarkably, we find no clear relationship between short-term sediment yields and MAP in our analysis (Fig. 3b), but the Dry sub-humid erosion peak identified in these prior studies is observed in our relationship between MAP and long-term erosion rates (Fig. 3a, 9). We found an immense amount of scatter in the sediment yield (short-term) erosion data, which precluded fitting any systematic relationship, yet the long-term erosion rates revealed a more striking visible pattern, similar to previous studies on short-term erosion. We suspect the scatter in our compiled sediment yield data for the USA results from two key factors. First, the short-term nature of sediment flux records makes it less likely that these records have captured the full range of sediment transport events, so they might be over- or under-representing extreme events at any particular site, leading to much more scatter overall (Kirchner et al., 2001; Singer and Dunne, 2004; Covault et al., 2013). Second, historical records of sediment flux are more likely to be influenced by anthropogenic impacts (Hooke, 2000; Wilkinson and Mcelroy, 2007; Kemp et al., 2020), which may scramble inherent erosion signals, thereby generating more variability in the compiled records. Of course, it is also possible that physiographic variability (tectonics, lithology, land cover, etc.) may play a role in creating this variability in sediment yields, but we would expect these factors to also affect long-term erosion rates. For example, analysis of topographic influences on short- and long-term erosion for the entire global database reveals stronger relationships between erosion and channel relief and slope for the long-term erosion data (Fig. 8). Again, the substantial scatter in the short-term erosion data suggests a scrambling of the signal, which is more coherent for long-term data.

Based on a more limited compilation of global ^{10}Be data, Mishra et al. (2019) found a similar relationship between long-term erosion rate and precipitation, albeit with differences in erosion peak locations that may be artefacts of their polynomial fit

(Fig. 9). Nevertheless, there is clear corroboration in data and theoretical underpinning supporting a peak in erosion rates within dry sub-humid landscapes near the transition from dry to wet precipitation regimes and sparse to extensive vegetation cover (Figs. 2b, 3a, 9; Molnar et al, 2006; Langbein and Schumm, 1958; Collins and Bras, 2008). We suggest that this relationship, originally posited for short-term erosion data, may be more evident in long-term erosion data (despite all the inherent uncertainties and biases in cosmogenic radionuclides) because the time averaging incorporates the cumulative effects of climate into the erosion rate.

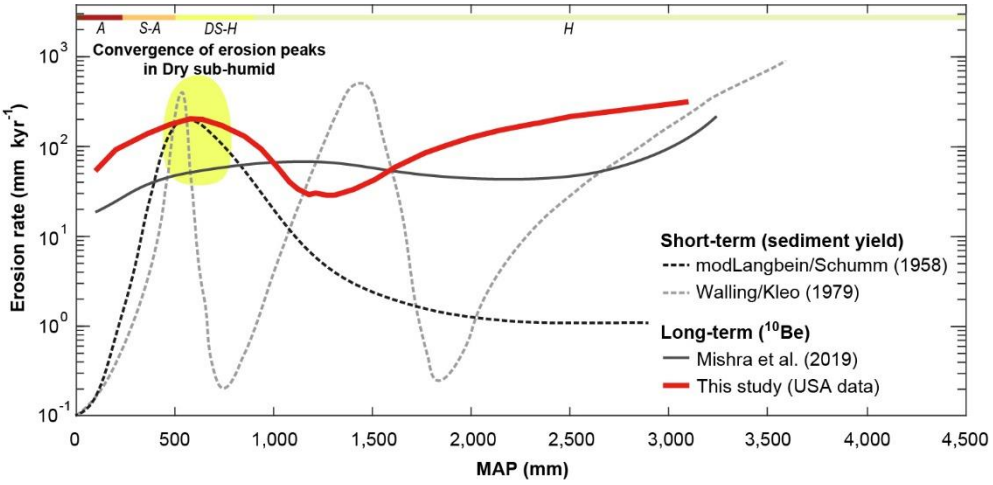

Figure 9: Synthesis of non-linear relationships between MAP and short-term erosion rates (modified Langbein and Schumm, 1958 (see text), and Walling and Kleo, 1979), and between MAP and long-term erosion rates (Mishra et al., 2019, and this study). MAP precipitation regimes akin to Aridity Index classes are shown along top. The figure highlights the convergence of erosion peaks in Dry sub-humid regions.

When erosion is averaged over timescales long enough to capture the effects of past glaciations, this signal appears to be detectable for high and mid-latitude regions, wherein formerly glaciated locations within the Temperate K–G climate zone exhibit erosion rates five times higher than unglaciated regions within this same climate zone (Fig. 4). This result is consistent with previous studies, which argued that in mid- and high-latitude regions, long-term erosion rates tend to be higher than low-latitude regions because glacial and periglacial processes during ice ages stripped away the underlying land surface and increased physical weathering through freeze–thaw processes (Schaller et al., 2002; Portenga and Bierman, 2011; Harel et al., 2016; Cook et al., 2020). Our result of higher erosion in regions with past glaciation is also consistent with the relatively low ratio of short- to long-term erosion for the Humid AI category (Fig. 2b), which likely arises in part because the Humid class includes 46% of the total number of formerly glaciated sites included in our analysis. The strength of this glacial signal in the data suggests that the effects on long-term erosion rates are real, even if there are potential uncertainties and biases in the cosmogenic radionuclide record spanning glacial periods (Ganti et al., 2016). Thus, the influence of glaciation may have contributed to observed higher long-term erosion rates than short-term rates in previous work (e.g. Kirchner et al., 2001)

When we compared long-term to short-term erosion rates, we found that short-term erosion rates are higher than long-term rates in all climate categories for both classifications, except for the K–G Cold zone (Fig. 2), which is mostly covered by contiguous boreal forest. This result may be surprising when viewed primarily through the lens of capturing extreme events because shorter records would be less likely to capture higher sediment yields in response to wildfires, earthquakes, etc. Therefore, the higher short-term erosion rates can only be reasonable viewed through the window of a recently more erosive environment due to the impact of humans globally. To test this notion, we classified short-term erosion rates by broad agricultural land-use categories (Foley et al., 2005) and found that erosion rates in both croplands and pastures/rangelands are similar and significantly higher than erosion rates for classes without anthropogenic influences (Fig. 5). These results support previous findings that human activities significantly increase short-term erosion rates, and that they are consistently detectable around the globe. Human activities have increased short-term erosion rates by an estimated one to two orders of magnitude (Milliman and Syvitski, 1992; Dedkov and Mozzherin, 1996; Montgomery, 2007; Wilkinson and Mcelroy, 2007; Kemp et al., 2020), suggesting that human influences on sediment yields outweigh natural processes (Hooke, 2000; Wilkinson and Mcelroy, 2007; Kemp et al., 2020). Among the many anthropogenic activities expressed on surface erosion around the globe, agriculture has one of the highest impacts on the land surface because it directly alters both vegetation through replacement of forest canopies with low-interception coverage crops, and soils through replacement of natural profiles containing developed organic layers with homogenised profiles that undergo cycles of tillage and surface compaction (Hooke, 2000). This anthropogenic disruption of vegetation and soils should create higher susceptibility to erosion by rainsplash, runoff, and wind (Dedkov and Mozzherin, 1996; Wilkinson and Mcelroy, 2007; Kemp et al., 2020), even in lowland environments. The eroded material would then contribute to stream channels, where it would be measured as systematically elevated sediment yields compared to pre-historic levels.

It is worth noting that the difference in short-term erosion rates between anthropogenic and non-anthropogenic regions shown here is smaller than was shown in previous studies (Dedkov and Mozzherin, 1996; Montgomery, 2007; Wilkinson and Mcelroy, 2007; Kemp et al., 2020). For example, Dedkov and Mozzherin (1996) estimated that anthropogenic activities increase sediment yields by a factor of 3.5 in large rivers and a factor of 8 in small rivers. We speculate that one of the main reasons for this discrepancy is that here we may be underestimating the amount of area that is influenced by anthropogenic activity, based on our defined threshold of > 50% agricultural area. Another possibility is that our analysis may be including more short-term erosion rates sampled in anthropogenically impacted regions, where substantial soil and water conservation efforts in upstream basins, as well as engineering structures (e.g. dams) that trap sediment may result in artificially lower sediment yields (Walling and Webb, 1996; Hooke, 2000; Walling and Fang, 2003; Syvitski et al., 2005; Wilkinson and Mcelroy, 2007; Singer and Dunne, 2006; Singer and Aalto, 2009).

Finally, we address the influence of inherent drainage basin characteristics on erosion rates, since this topic has proliferated in the literature about erosion due to the spatially variable influence of tectonics, lithology, and vegetation cover. Since this study was not specifically focused on these basin drivers of erosion (but rather on climate and anthropogenic drivers), we merely explored the influence of channel relief and slope on short- and long-term erosion rates, since they reflect both the local tectonic uplift history and the lithology. Separately, we investigated whether drainage basin area influences erosion rates. We found positive relationships between both channel gradient and total channel relief and long-term erosion rates (Fig. 8a, b), yet there was no clear relationship between short-term erosion rates and these topographic indices (Fig. 8c, d). Drainage basin steepness is considered a critical control on erosion rates (e.g. Summerfield and Hulton, 1994; Granger et al., 1996; Portenga and Bierman, 2011), which is also fundamental to the stream power incision law. Drainage basins with higher steepness tend to produce higher velocity of runoff because of the downslope vector of potential energy, which increases the shear stress of water flow and thus produces higher erosion that shapes land surface and transports sediments downstream (Knighton, 1998; Whipple and Tucker, 1999). In addition, steep drainage basins are often located in tectonically active regions, with low bedrock strength, high frequency of landslides (Binnie et al., 2007; Grin et al., 2018), and high precipitation rates induced by orography (Willett, 1999; Roe et al., 2002), all of which would tend to increase erosion rates. Therefore, it is logical that there would be a strong relationship between topography and erosion (as shown previously in many studies), yet it is less obvious why short-term rates do not exhibit this relationship. One possibility is that agriculture, a key anthropogenic influence on erosion, tends to cluster in downstream parts of drainage basins with gentler slopes (Wilkinson and Mcelroy, 2007). In upstream sections of drainage basins, anthropogenic activities that accelerate erosion (e.g. deforestation) may be ameliorated (from a sediment yield perspective) by soil and water conservation efforts (Montgomery, 2007), and/or by the trapping of sediment within reservoirs (Walling and Webb, 1996; Walling and Fang, 2003; Syvitski et al., 2005). Thus, sediment yields may vary substantially from upstream to downstream even within the same basin, depending on the locations of these anthropogenic activities within the landscape, as well as cycles of erosion, deposition, and remobilisation, which would lead to a scrambling of the relationship between topography and erosion (Fig. 8d).

We further investigated short- and long-term erosion rates categorised by basin area but found no clear relationship between basin area and long-term or short-term erosion rates within our compiled global dataset (Fig. 6). Stream power incision law predicts a positive relationship between basin area and erosion rate because the former is often positively related to water discharge that exerts erosive power on the land surface (Whipple et al., 1999). However, some studies present an inverse relationship between these factors (e.g. Milliman and Syvitski, 1992; Milliman and Farnsworth, 2011), whilst others found no clear relationship (e.g. Summerfield and Hulton, 1994; Kirchner et al., 2001; DiBiase et al., 2010). There are several factors that potentially obscure any systematic relationship between basin area and erosion including the sampling location within the basin, tectonic setting, and underlying lithology. Apparently, the effect of basin area alone on either short- or long-term erosion rates is not detectable because it is obscured by the various other controls. However, when we classified the ratio of short- to long-term erosion rates, $R_{S/L}$, by basin area, we found a negative relationship for each of the K–G climate zones, except the

Cold zone (Fig. 7). Prior work has shown that in large basins, the differences between long- and short-term erosion rates are less discernible compared to small basins, due to the sediment buffering capacity of large drainage basins (Wittmann et al., 2011; Covault et al., 2013). Buffering capacity is determined by the balance between sediment supply and the accommodation space for deposition (Wittmann et al., 2011; Covault et al., 2013), favoring larger basins. Notably, the $R_{S/L}$ values are less sensitive to basin area within arid catchments compared to more humid zones (Fig. 7) because arid regions have a distinctive hydrological regime, where storms tend to have shorter duration, smaller spatial coverage, and high spatial variability, which generate partial area runoff (Yair et al., 1978; Singer and Michaelides, 2017; Michaelides et al., 2018). Arid regions also experience transmission losses within porous river channels, resulting in a breakdown in the relationship between basin area and streamflow, compared to the positive relationship found in humid regions (Knighton and Nanson, 1997; Tooth, 2000; Singer and Michaelides, 2014; Jaeger et al., 2017). These characteristic features of arid zone hydrology reduce the influence of basin area on hydrological processes, including sediment yields, leading to weaker buffering capacity of drainage basins in arid regions. An additional factor that may explain the lack of area control in arid regions is that short-term erosion rates tend to be systematically higher than long-term rates (Gellis et al., 2004; Bierman et al., 2005), which creates values of $R_{S/L}$ closer to unity, regardless of basin size. In tropical regions, the $R_{S/L}$ values are generally higher than other climate zones, which may result from lower long-term erosion rates compared to Temperate and Cold zones (perhaps due to the lack of past glaciation), and higher short-term erosion rates due to intensive agricultural activity which may destroy the dense vegetation cover (e.g. deforestation), although the ratio declines substantially with basin size (Fig. 7). In the Temperature and Cold K–G zones, the $R_{S/L}$ values are generally lower than the other two categories (i.e. long-term erosion rates are more similar to short-term rates, or even higher) likely because glacial and periglacial processes since the LGM led to increased long-term rates.

6 Conclusions

By compiling and analysing erosion rates from globally distributed sites, we demonstrate a few key differences in long- and short-term rates and their dominant controls: 1) short-term erosion rates are significantly higher than long-term erosion rates in all climate zones except in the K–G Cold zone; 2) long-term erosion rates are higher in mid- and high-latitude regions (including the K–G Cold zone and part of the Temperate zone), likely due to glacial and periglacial processes during past ice ages; 3) only long-term erosion rates are strongly related to indices of climate and topography, whilst short-term rates exhibit a scrambled signal with high variability; and 4) short-term erosion rates seem to be dominated by human activities which mask natural controls. A key finding is that a relationship exists between long-term erosion rates and climate showing a peak in the Dry sub-humid rainfall regime, which reflects the balance between precipitation and vegetation cover. However, this relationship does not hold for the short-term erosion rates analysed here, in contrast to the results presented in prior studies (Langbein and Schumm, 1958; Walling and Kleo, 1979). Finally, we show that short-term erosion rates are generally several times higher than long-term rates in small basins, showing that human-induced erosion is more detectable in small basins with

lower sediment buffering capacity, whilst long-term erosion rates tend to be similar or even higher than short-term rates in large basins.

Data availability.

Short-term erosion rate data from compiled sediment fluxes are available at the University of Bristol data repository, data.bris, at https://doi.org/10.5523/bris.1pq50eh0902da25aps5nhc1ngv.

Author contribution.

All authors contributed to the design, interpretation, and write-up of the study. S.-A.C. carried out the data compilation and data analyses.

Competing interests.

The authors declare that they have no conflict of interest.

References

Aalto, R., Dunne, T., and Guyot, J. L.: Geomorphic controls on Andean denudation rates, J. Geol., 114, 85–99, https://doi.org/10.1086/498101, 2006.

Alexandrov, Y., Cohen, H., Laronne, J. B., and Reid, I.: Suspended sediment load, bed load, and dissolved load yields from a semiarid drainage basin: A 15-year study, Water Resour. Res., 45, W08408, https://doi.org/10.1029/2008WR007314, 2009.

Asner, G. P., Elmore, A. J., Olander, L. P., Martin, R. E., and Harris, A. T.: Grazing systems, ecosystem responses, and global change, Annu. Rev. Environ. Resour., 29, 261–299, https://doi.org/10.1146/annurev.energy.29.062403.102142, 2004.

Bierman, P. R., and Caffee, M.: Slow rates of rock surface erosion and sediment production across the Namib Desert and escarpment, southern Africa, Am. J. Sci., 301, 326–358, https://doi.org/10.2475/ajs.301.4-5.326, 2001.

Bierman, P. R., Reuter, J. M., Pavich, M., Gellis, A. C., Caffee, M. W., and Larsen, J.: Using cosmogenic nuclides to contrast rates of erosion and sediment yield in a semi-arid, arroyo-dominated landscape, Rio Puerco Basin, New Mexico, Earth Surf. Process. Landf., 30, 935–953, https://doi.org/10.1002/esp.1255, 2005.

Binnie, S. A., Phillips, W. M., Summerfield, M. A., and Fifield, L. K.: Tectonic uplift, threshold hillslopes, and denudation rates in a developing mountain range, Geology, 35, 743–746, https://doi.org/10.1130/G23641A.1, 2007.

Brown, E. T., Stallard, R. F., Larsen, M. C., Raisbeck, G. M., and Yiou, F.: Denudation rates determined from the accumulation of in situ-produced ^{10}Be in the Luquillo Experimental Forest, Puerto Rico, Earth Planet. Sci. Lett., 129, 193–202, https://doi.org/10.1016/0012-821X(94)00249-X, 1995.

Cannon, S. H., Powers, P. S., and Savage, W. Z.: Fire-related hyperconcentrated and debris flows on Storm King Mountain, Glenwood Springs, Colorado, USA, Environ. Geol., 35, 210–218, https://doi.org/10.1007/s002540050307, 1998.

Chen, S.-A., Michaelides, K., Grieve, S. W. D., and Singer, M. B.: Aridity is expressed in river topography globally, Nature, 573, 573–577, https://doi.org/10.1038/s41586-019-1558-8, 2019.

Clapp, E. M., Bierman, P. R., Nichols, K. K., Pavich, M., and Caffee, M.: Rates of sediment supply to arroyos from upland erosion determined using in situ produced cosmogenic ^{10}Be and ^{26}Al, Quat. Res., 55, 235–245, https://doi.org/10.1006/qres.2000.2211, 2001.

Clapp, E. M., Bierman, P. R., Schick, A. P., Lekach, J., Enzel, Y., and Caffee, M.: Sediment yield exceeds sediment production in arid region drainage basins, Geology, 28, 995–998, https://doi.org/10.1130/0091-7613(2000)28<995:SYESPI>2.0.CO;2, 2000.

Cleveland, W. S.: Robust locally weighted regression and smoothing scatterplots, J. Am. Stat. Assoc., 74, 829–836, https://doi.org/10.1080/01621459.1979.10481038, 1979.

Codilean, A. T., Fenton, C. R., Fabel, D., Bishop, P., and Xu, S.: Discordance between cosmogenic nuclide concentrations in amalgamated sands and individual fluvial pebbles in an arid zone catchment, Quat. Geochronol., 19, 173–180, https://doi.org/10.1016/j.quageo.2012.04.007, 2014.

Codilean, A. T., Munack, H., Cohen, T. J., Saktura, W. M., Gray, A. G., and Mudd, S. M.: OCTOPUS: an open cosmogenic isotope and luminescence database, Earth Syst. Sci. Data, 10, 2123–2139, https://doi.org/10.5194/essd-10-2123-2018, 2018.

Collins, D. B. G., and Bras, R. L.: Climatic control of sediment yield in dry lands following climate and land cover change, Water Resour. Res., 44, W10405, https://doi.org/10.1029/2007WR006474, 2008.

Cook, S. J., Swift, D. A., Kirkbride, M. P., Knight, P. G., and Waller, R. I.: The empirical basis for modelling glacial erosion rates, Nat. Commun., 11, 759, https://doi.org/10.1038/s41467-020-14583-8, 2020.

Covault, J. A., Craddock, W. H., Romans, B. W., Fildani, A., and Gosai, M.: Spatial and temporal variations in landscape evolution: historic and longer-term sediment flux through global catchments, J. Geol., 121, 35–56, https://doi.org/10.1086/668680, 2013.

Dedkov, A. P., and Mozzherin, V. I.: Erosion and sediment yield on the Earth, in: Erosion and Sediment Yield: Global and Regional Perspectives, edited by: Walling, D. E., and Webb, B. W., IAHS Publications, Wallingford, Oxfordshire, UK, 236, 29–36, 1996.

Delunel, R., Schlunegger, F., Valla, P. G., Dixon, J., Glotzbach, C., Hippe, K., Kober, F., Molliex, S., Norton, K. P., Salcher, B., Wittmann, H., Akçar, N., and Christl, M.: Late-Pleistocene catchment-wide denudation patterns across the European Alps, Earth-Sci. Rev., 211, 103407, https://doi.org/10.1016/j.earscirev.2020.103407, 2020.

DiBiase, R. A., Whipple, K. X., Heimsath, A. M., and Ouimet, W. B.: Landscape form and millennial erosion rates in the San Gabriel Mountains, CA, Earth Planet. Sci. Lett., 289, 134–144, https://doi.org/10.1016/j.epsl.2009.10.036, 2010.

Dosseto, A., and Schaller, M.: The erosion response to Quaternary climate change quantified using uranium isotopes and in situ-produced cosmogenic nuclides, Earth-Sci. Rev., 155, 60–81, https://doi.org/10.1016/j.earscirev.2016.01.015, 2016.

Dunne, T., and Leopold, L. B.: Water in Environmental Planning, Freeman, New York, US, 1978.

Foley, J. A., DeFries, R., Asner, G. P., Barford, C., Bonan, G., Carpenter, S. R., Chapin, F. S., Coe, M. T., Daily, G. C., and Gibbs, H. K.: Global consequences of land use, Science, 309, 570–574, https://doi.org/10.1126/science.1111772, 2005.

Ganti, V., von Hagke, C., Scherler, D., Lamb, M. P., Fischer, W. W., and Avouac, J.-P.: Time scale bias in erosion rates of glaciated landscapes, Sci. Adv., 2, e1600204, https://doi.org/10.1126/sciadv.1600204, 2016.

Gellis, A. C., Pavich, M. J., Bierman, P. R., Clapp, E. M., Ellevein, A., and Aby, S.: Modern sediment yield compared to geologic rates of sediment production in a semi-arid basin, New Mexico: assessing the human impact, Earth Surf. Process. Landf., 29, 1359–1372, https://doi.org/10.1002/esp.1098, 2004.

Granger, D. E., Kirchner, J. W., and Finkel, R.: Spatially averaged long-term erosion rates measured from in situ-produced cosmogenic nuclides in alluvial sediment, J. Geol., 104, 249–257, https://doi.org/10.1086/629823, 1996.

Granger, D. E., Lifton, N. A., and Willenbring, J. K.: A cosmic trip: 25 years of cosmogenic nuclides in geology, GSA Bull., 125, 1379–1402, https://doi.org/10.1130/B30774.1, 2013.

Granger, D. E., and Schaller, M.: Cosmogenic nuclides and erosion at the watershed scale, Elements, 10, 369–373, https://doi.org/10.2113/gselements.10.5.369, 2014.

Grin, E., Schaller, M., and Ehlers, T. A.: Spatial distribution of cosmogenic ^{10}Be derived denudation rates between the Western Tian Shan and Northern Pamir, Tajikistan, Geomorphology, 321, 1–15, https://doi.org/10.1016/j.geomorph.2018.08.007, 2018.

Harel, M.-A., Mudd, S. M., and Attal, M.: Global analysis of the stream power law parameters based on worldwide ^{10}Be denudation rates, Geomorphology, 268, 184–196, https://doi.org/10.1016/j.geomorph.2016.05.035, 2016.

Hilley, G. E., Porder, S., Aron, F., Baden, C. W., Johnstone, S. A., Liu, F., Sare, R., Steelquist, A., and Young, H. H.: Earth's topographic relief potentially limited by an upper bound on channel steepness, Nat. Geosci., 12, 828–832, https://doi.org/10.1038/s41561-019-0442-3, 2019.

Hooke, R. L.: On the history of humans as geomorphic agents, Geology, 28, 843–846, https://doi.org/10.1130/0091-7613(2000)28<843:OTHOHA>2.0.CO;2, 2000.

Istanbulluoglu, E. and Bras, R. L.: On the dynamics of soil moisture, vegetation, and erosion: Implications of climate variability and change, Water Resour. Res., 42, W06418, https://doi.org/10.1029/2005WR004113, 2006.

Jaeger, K. L., Sutfin, N. A., Tooth, S., Michaelides, K., and Singer, M.: Geomorphology and sediment regimes of intermittent rivers and ephemeral streams, in: Intermittent Rivers and Ephemeral Streams: Ecology and Management, edited by: Datry, T., Bonada, N., and Boulton, A., Elsevier, 21–49, https://doi.org/10.1016/B978-0-12-803835-2.00002-4, 2017.

Kemp, D. B., Sadler, P. M., and Vanacker, V.: The human impact on North American erosion, sediment transfer, and storage in a geologic context, Nat. Commun., 11, 6012, https://doi.org/10.1038/s41467-020-19744-3, 2020.

Kirchner, J. W., Finkel, R. C., Riebe, C. S., Granger, D. E., Clayton, J. L., King, J. G., and Megahan, W. F.: Mountain erosion over 10 yr, 10 k.y., and 10 m.y. time scales, Geology, 29, 591–594, https://doi.org/10.1130/0091-7613(2001)029<0591:MEOYKY>2.0.CO;2, 2001.

Knighton, A., and Nanson, G.: Distinctiveness, diversity and uniqueness in arid zone river systems, in: Arid Zone Geomorphology: Process, Form and Change in Drylands, second edition, edited by: Thomas, D. S. G., John Wiley & Sons, Chichester, West Sussex, UK, 185–203, 1997.

Knighton, D.: Fluvial Forms and Processes: A New Perspective, Edward Arnold, London, UK, 1998.

Langbein, W. B., and Schumm, S. A.: Yield of sediment in relation to mean annual precipitation, Eos, Trans. AGU, 39, 1076–1084, https://doi.org/10.1029/TR039i006p01076, 1958.

Leopold, L. B., Wolman, M. G., and Miller, J. P.: Fluvial Processes in Geomorphology, Freeman, San Francisco, US, 1964.

Meyer, G. A., Pierce, J. L., Wood, S. H., and Jull, A. J. T.: Fire, storms, and erosional events in the Idaho batholith, Hydrol. Process., 15, 3025–3038, https://doi.org/10.1002/hyp.389, 2001.

Michaelides, K., Hollings, R., Singer, M. B., Nichols, M. H., and Nearing, M. A.: Spatial and temporal analysis of hillslope–channel coupling and implications for the longitudinal profile in a dryland basin, Earth Surf. Process. Landf., 43, 1608–1621, https://doi.org/10.1002/esp.4340, 2018.

Milliman, J. D., and Farnsworth, K. L. (Eds.): River Discharge to the Coastal Ocean: A Global Synthesis, Cambridge University Press, Cambridge, UK, 2011.

Milliman, J. D., and Farnsworth, K. L. (Eds.): River Discharge to the Coastal Ocean: A Global Synthesis, Cambridge University Press, Cambridge, UK, 2013.

Milliman, J. D., and Meade, R. H.: World-wide delivery of river sediment to the oceans, J. Geol., 91, 1–21, https://doi.org/10.1086/628741, 1983.

Milliman, J. D., and Syvitski, J. P.: Geomorphic/tectonic control of sediment discharge to the ocean: the importance of small mountainous rivers, J. Geol., 100, 525–544, https://doi.org/10.1086/629606, 1992.

Mishra, A. K., Placzek, C., and Jones, R.: Coupled influence of precipitation and vegetation on millennial-scale erosion rates derived from ^{10}Be, PloS One, 14, e0211325, https://doi.org/10.1371/journal.pone.0211325, 2019.

Molnar, P., Anderson, R. S., Kier, G., and Rose, J.: Relationships among probability distributions of stream discharges in floods, climate, bed load transport, and river incision, J. Geophys. Res. Earth Surf., 111, F02001, https://doi.org/10.1029/2005JF000310, 2006.

Montgomery, D. R.: Soil erosion and agricultural sustainability, Proc. Natl. Acad. Sci., 104, 13268–13272, https://doi.org/10.1073/pnas.0611508104, 2007.

NOAA PSL, Boulder, Colorado, USA, CPC US Unified Precipitation data, https://psl.noaa.gov, last access: 13 January 2020.

Pan, B.-T., Geng, H.-P., Hu, X.-F., Sun, R.-H., and Wang, C.: The topographic controls on the decadal-scale erosion rates in Qilian Shan Mountains, N.W. China, Earth Planet. Sci. Lett., 292, 148–157, https://doi.org/10.1016/j.epsl.2010.01.030, 2010.

Peel, M. C., Finlayson, B. L., and McMahon, T. A.: Updated world map of the Köppen-Geiger climate classification, Hydrol. Earth Syst. Sci. Discuss., 4, 439–473, https://hal.archives-ouvertes.fr/hal-00298818, 2007.

Pierce, J. L., Meyer, G. A., and Jull, A. J. T.: Fire-induced erosion and millennial-scale climate change in northern ponderosa pine forests, Nature, 432, 87–90, https://doi.org/10.1038/nature03058, 2004.

Portenga, E. W., and Bierman, P. R.: Understanding Earth's eroding surface with ^{10}Be, GSA Today, 21, 4–10, https://doi.org/10.1130/G111A.1, 2011.

Ramankutty, N., and Foley, J. A.: Estimating historical changes in global land cover: Croplands from 1700 to 1992, Global Biogeochem. Cycles, 13, 997–1027, https://doi.org/10.1029/1999GB900046, 1999.

Ray, N., and Adams, J.: A GIS-based vegetation map of the world at the Last Glacial Maximum (25,000-15,000 BP), Internet Archaeol., 11, https://archive-ouverte.unige.ch/unige:17817, 2001.

Roe, G. H., Montgomery, D. R., and Hallet, B.: Effects of orographic precipitation variations on the concavity of steady-state river profiles, Geology, 30, 143–146, https://doi.org/10.1130/0091-7613(2002)030<0143:EOOPVO>2.0.CO;2, 2002.

Schaller, M., von Blanckenburg, F., Hovius, N., and Kubik, P.: Large-scale erosion rates from in situ-produced cosmogenic nuclides in European river sediments, Earth Planet. Sci. Lett., 188, 441–458, https://doi.org/10.1016/S0012-821X(01)00320-X, 2001.

Schaller, M., von Blanckenburg, F., Veldkamp, A., Tebbens, L., Hovius, N., and Kubik, P.: A 30 000 yr record of erosion rates from cosmogenic ^{10}Be in Middle European river terraces, Earth Planet. Sci. Lett., 204, 307–320, https://doi.org/10.1016/S0012-821X(02)00951-2, 2002.

Schmidt, A. H., Neilson, T. B., Bierman, P. R., Rood, D. H., Ouimet, W. B., and Gonzalez, V. S.: Influence of topography and human activity on apparent in situ ^{10}Be-derived erosion rates in Yunnan, SW China, Earth Surf. Dynam., 4, 819–830, http://dx.doi.org/10.5194/esurf-4-819-2016, 2016.

Singer, M. B., and Aalto, R.: Floodplain development in an engineered setting, Earth Surf. Process. Landf., 34, 291–304, https://doi.org/10.1002/esp.1725, 2009.

Singer, M. B., and Dunne, T.: Modeling decadal bed material sediment flux based on stochastic hydrology, Water Resour. Res., 40, W03302, https://doi.org/10.1029/2003WR002723, 2004.

Singer, M. B., and Dunne, T.: Modeling the influence of river rehabilitation scenarios on bed material sediment flux in a large river over decadal timescales, Water Resour. Res., 42, W12415, https://doi.org/10.1029/2006WR004894, 2006.

Singer, M. B., and Michaelides, K.: How is topographic simplicity maintained in ephemeral dryland channels?, Geology, 42, 1091–1094, https://doi.org/10.1130/G36267.1, 2014.

Singer, M. B., and Michaelides, K.: Deciphering the expression of climate change within the Lower Colorado River basin by stochastic simulation of convective rainfall, Environ. Res. Lett., 12, 104011, https://doi.org/10.1088/1748-9326/aa8e50, 2017.

Struck, M., Jansen, J. D., Fujioka, T., Codilean, A. T., Fink, D., Fülöp, R.-H., Wilcken, K. M., Price, D. M., Kotevski, S., and Fifield, L. K.: Tracking the ^{10}Be–^{26}Al source-area signal in sediment-routing systems of arid central Australia, Earth Surf. Dynam., 6, 329–349, https://doi.org/10.5194/esurf-6-329-2018, 2018.

Summerfield, M., and Hulton, N.: Natural controls of fluvial denudation rates in major world drainage basins, J. Geophys. Res. Solid Earth., 99, 13871–13883, https://doi.org/10.1029/94JB00715, 1994.

Syvitski, J. P., and Milliman, J. D.: Geology, geography, and humans battle for dominance over the delivery of fluvial sediment to the coastal ocean, J. Geol., 115, 1–19, https://doi.org/10.1086/509246, 2007.

Syvitski, J. P., Vörösmarty, C. J., Kettner, A. J., and Green, P.: Impact of humans on the flux of terrestrial sediment to the global coastal ocean, Science, 308, 376–380, https://doi.org/10.1126/science.1109454, 2005.

Tofelde, S., Duesing, W., Schildgen, T. F., Wickert, A. D., Wittmann, H., Alonso, R. N., and Strecker, M.: Effects of deep-seated versus shallow hillslope processes on cosmogenic ^{10}Be concentrations in fluvial sand and gravel, Earth Surf. Process. Landf., 43, 3086–3098, https://doi.org/10.1002/esp.4471, 2018.

Tooth, S.: Process, form and change in dryland rivers: a review of recent research, Earth Sci. Rev., 51, 67–107, https://doi.org/10.1016/S0012-8252(00)00014-3, 2000.

Trabucco, A., and Zomer, R. J.: Global Aridity and PET Database, CGIAR Consortium for Spatial Information, http://www.cgiar-csi.org/data/global-aridity-and-pet-database, 2009.

U.S. Geological Survey, National Water Information System data available on the World Wide Web (USGS Water Data for the Nation): https://waterdata.usgs.gov/nwis, last access: 2 December 2019.

von Blanckenburg, F.: The control mechanisms of erosion and weathering at basin scale from cosmogenic nuclides in river sediment, Earth Planet. Sci. Lett., 237, 462–479, https://doi.org/10.1016/j.epsl.2005.06.030, 2006.

von Blanckenburg, F., and Willenbring, J. K.: Cosmogenic nuclides: dates and rates of Earth-surface change, Elements, 10, 341–346, https://doi.org/10.2113/gselements.10.5.341, 2014.

Walling, D., and Fang, D.: Recent trends in the suspended sediment loads of the world's rivers, Global Planet. Change, 39, 111–126, https://doi.org/10.1016/S0921-8181(03)00020-1, 2003.

Walling, D., and Webb, B.: Erosion and sediment yield: a global overview, in: Erosion and Sediment Yield: Global and Regional Perspectives, edited by: Walling, D. E., and Webb, B. W., IAHS Publications, Wallingford, Oxfordshire, UK, 236, 3–20, 1996.

Walling, D. E., and Kleo, A. H. A.: Sediment yields of rivers in areas of low precipitation: a global view, in: The Hydrology of Areas of Low Precipitation, IAHS Publications, Wallingford, Oxfordshire, UK, 128, 479–493, 1979.

Whipple, K. X., Kirby, E., and Brocklehurst, S. H.: Geomorphic limits to climate-induced increases in topographic relief, Nature, 401, 39–43, https://doi.org/10.1038/43375, 1999.

Whipple, K. X., and Tucker, G. E.: Dynamics of the stream-power river incision model: Implications for height limits of mountain ranges, landscape response timescales, and research needs, J. Geophys. Res. Solid Earth, 104, 17661–17674, https://doi.org/10.1029/1999JB900120, 1999.

Wilkinson, B. H., and McElroy, B. J.: The impact of humans on continental erosion and sedimentation, GSA Bull., 119, 140–156, https://doi.org/10.1130/B25899.1, 2007.

Willett, S. D.: Orogeny and orography: The effects of erosion on the structure of mountain belts, J. Geophys. Res. Solid Earth, 104, 28957–28981, https://doi.org/10.1029/1999JB900248, 1999.

Wittmann, H., von Blanckenburg, F., Maurice, L., Guyot, J.-L., Filizola, N., and Kubik, P. W.: Sediment production and delivery in the Amazon River basin quantified by in situ–produced cosmogenic nuclides and recent river loads, GSA Bull., 123, 934–950, https://doi.org/10.1130/B30317.1, 2011.

Yair, A., Sharon, D., and Lavee, H.: An instrumented watershed for the study of partial area contribution of runoff in the arid zone, Z. Geomorphol. Suppl., 29, 71–82, 1978.

Yizhou, W., Huiping, Z., Dewen, Z., Wenjun, Z., Zhuqi, Z., Weitao, W., and Jingxing, Y.: Controls on decadal erosion rates in Qilian Shan: re-evaluation and new insights into landscape evolution in north-east Tibet, Geomorphology, 223, 117–128, https://doi.org/10.1016/j.geomorph.2014.07.002, 2014.